Increased hippocampal CA1 cerebral blood volume in schizophrenia

Pratik Talati [*,a,b], Swati Rane[c], Samet Kose[b], Jennifer Urbano Blackford[b], John Gore[c], Manus J. Donahue[b,c], Stephan Heckers[b]

[a]Vanderbilt Brain Institute, Vanderbilt University, Nashville, TN 37235, USA
[b]Department of Psychiatry, Vanderbilt University, Nashville, TN 37235, USA
[c]Department of Radiology and Radiological Sciences, Institute of Imaging Science, Vanderbilt University, Nashville, TN 37235, USA

ARTICLE INFO

ABSTRACT

Hippocampal hyperactivity has been proposed as a biomarker in schizophrenia. However, there is a debate whether the CA1 or the CA2/3 subfield is selectively affected. We studied 15 schizophrenia patients and 15 matched healthy control subjects with 3T steady state, gadolinium-enhanced, absolute cerebral blood volume (CBV) maps, perpendicular to the long axis of the hippocampus. The subfields of the hippocampal formation (subiculum, CA1, CA2/3, and hilus/dentate gyrus) were manually segmented to establish CBV values. Comparing anterior CA1 and CA2/3 CBV between patients and controls revealed a significant subfield-by-diagnosis interaction. This interaction was due to the combined effect of a trend of increased CA1 CBV ($p = .06$) and non-significantly decreased CA2/3 CBV ($p = 0.14$) in patients relative to healthy controls. These results support the emerging hypothesis of increased hippocampal activity as a biomarker of schizophrenia and highlight the importance of subfield-level investigations.

1. Introduction

The hippocampus is dysfunctional in schizophrenia (Weiss, 2003; Ongür, 2006; Ragland, 2001; Ledoux, 2013; Heckers, and Konradi, 2010). Meta-analyses have concluded that schizophrenia is associated with memory impairment (Heinrichs, and Zakzanis, 1998; Aleman, 1999) and that hippocampal recruitment is impaired during the performance of memory tasks (Weiss, 2003; Heckers, 1998). However, a notable limitation of such functional studies is that individuals with cognitive deficits may have difficulty performing tasks in a scanning environment.

To circumvent issues associated with cognitive deficits and the limits in the interpretation of neural origins of the BOLD signal (Arthurs, and Boniface, 2002), several investigators have measured baseline hippocampal activity using non-BOLD methods. Initial baseline 18F-deoxyglucose positron emission tomography (PET) studies of medial temporal lobe activity in schizophrenia provided mixed results (i.e., decreased (Nordahl, 1996; Tamminga, 1992) or increased (DeLisi, 1989; Gur, 1995) in schizophrenia). However, several 15O-PET and Single Photon Emission Computed Tomography (SPECT) studies of regional cerebral blood flow (CBF) have established increased hippocampal baseline activity in schizophrenia (Heckers, 1998; Lahti, 2009; Lahti, 2003; Friston, 1992; Malaspina, 2004). A recent resting-state BOLD fMRI study revealed greater right hippocampal activity in schizophrenia by measuring intrinsic signal intensity fluctuations (Tregellas, 2014).

Hippocampal hyperactivity has been proposed as a biomarker for schizophrenia (Tregellas, 2014), but it is unclear whether it affects all hippocampal subfields. An initial study by Schobel reported increased cerebral blood volume (CBV) in subfield CA1 only (Schobel, 2009). This finding was limited to a single slice of the hippocampal formation, averaged across the right and the left hemisphere. A follow-up study by the same group explored CBV changes along the long axis of the hippocampal formation in a cohort at high risk for psychosis and demonstrated that increased left anterior CA1 CBV spreads to the subiculum after psychosis onset (Schobel, et al., 2013).

In contrast, Tamminga predicted increased CBV in the CA3 subfield, as the downstream result of dentate gyrus pathology (Tamminga, 2012). This model initially emerged as a way to bring together several findings in schizophrenia: smaller hippocampal volume, impaired activation during declarative memory tasks, increased baseline hippocampal perfusion, and reduced dentate gyrus neurogenesis and efferent signaling (Tamminga, Stan, and Wagner, 2010). They hypothesized that reduced pattern separation (i.e., the ability to distinguish between

* Corresponding author: Vanderbilt University, Department of Psychiatry, 3057 VPH, 1601 21st Ave South, Nashville, TN 37212, USA.
E-mail address: Pratik.talati@vanderbilt.edu (P. Talati).

similar events at different time periods) and greater pattern completion (i.e., the retrieval of information based on partial cues) result in the production and retrieval of incorrectly coded memories, leading to psychosis.

Taken together, the two competing models predict increased CBV either in CA1 or CA2/3.

Here we performed high spatial resolution, contrast-enhanced, T1-weighted steady state MRI in patients with schizophrenia and healthy controls to test these two opposing models of subfield-specific hyperactivity in the anterior hippocampus in schizophrenia. This method provides the necessary high spatial (sub-millimeter) resolution to parse out subfields of the hippocampal formation (Small, 2011) and has been implemented in our lab to characterize CBV gradients in different subfields (Talati, 2014).

2. Methods

2.1. Participants

15 healthy subjects and 15 patients with schizophrenia or schizoaffective disorder provided informed consent in a manner approved by the Vanderbilt Institutional Review Board. Patients and healthy controls were group-matched on age, gender, race, education, and parental education. Subjects were recruited from the Vanderbilt Psychotic Disorders Program or the local community and were paid for their participation. All subjects underwent a Structural Clinical Interview for DSM-IV Axis I disorders (SCID, (First et al., 2002)) to confirm the diagnosis, and healthy controls had no major psychiatric, neurological, or medical illness. Serum creatinine was measured in all participants before and after contrast administration to minimize the potential risk of nephrogenic systemic fibrosis.

2.2. Cerebral blood volume mapping

A Phillips 3T Achieva scanner with an 8 channel SENSE head coil was used for imaging. A 3D T1 FFE sequence (Lin, Celik, and Paczynski, 1999) was implemented to acquire T1-weighted pre- and post-contrast images with the following parameters: TR = 20 ms, TE = 3.98 ms, Field-of-View = 256 × 256 mm^2, Spatial resolution = 0.80 × 0.80 × 4 mm^3, slices = 30, SENSE factor = 2.5. A power injector (Medrad®, PA, USA) was used for contrast administration (Magnevist® − Gadopentate dimeglumine, Bayer Schering Pharma, Germany, 0.1 mmol/kg) and subsequent 40 ml saline flush through an 18G needle in the antecubital vein. After contrast administration, post-contrast images were acquired approximately 4 min later. To allow for accurate segmentation of the hippocampal subfields (Moreno, 2007), images were acquired perpendicular to the long axis of the hippocampus. For each subfield, the regions of interest (ROIs) were centered to avoid border regions with neighboring subfields. We compared the fractional increase in tissue signal after the contrast agent had thoroughly perfused the microvasculature and equilibrated in the blood.

2.3. Analysis

2.3.1. CBV calculations

AFNI (Cox, 1996) was used to correct for subject motion in pre- and post-contrast steady state images. Absolute CBV (units = ml blood/ml parenchyma) was calculated using the following equation:

$$CBV = \frac{S_{par,post} - S_{par,pre}}{S_{ss,post} - S_{ss,pre}} \times 100 \qquad (1)$$

where $S_{par,post} - S_{par,pre}$ is the difference between the post- and pre-contrast signals in the parenchyma and $S_{ss,post} - S_{ss,pre}$ denotes the difference between the post- and pre-contrast signals in the superior sagittal sinus (Lin, Celik, and Paczynski, 1999). To minimize

contribution from large epicortical vessels, a 10% regional CBV threshold was used (i.e., voxels with CBV values greater than 10 were excluded) (Lin, Celik, and Paczynski, 1999).

2.3.2. Hippocampal segmentation

The T1-weighted pre-contrast image was used for manual segmentation of the allocortical subfields of the hippocampal formation: subiculum, CA1, CA2/3, and hilus/dentate gyrus (referred to here as dentate gyrus) (Gloor, 1997). The post-contrast image was used to exclude large epicortical vessels. From manual segmentation, 5 ROIs were generated for each slice: hippocampal formation, subiculum, CA1, CA2/3, and dentate gyrus. All segmentations were performed by one blinded rater (PT) and verified by another blinded rater (SR). If there were any discrepancies, the ROI was drawn by both raters until a consensus was reached.

The uncus is defined in coronal sections as more than one cut through the hippocampal formation and was used to delineate between the anterior and posterior regions (Woolard, and Heckers, 2012; Duvernoy, and Bourgouin, 1998). The coronal series for each subject was numbered and aligned across all subjects using the presence or absence of the uncus as a guide. From this method, three slices (slices two–four) were labeled as anterior and three slices (slices five–seven) were labeled as posterior for the whole hippocampal formation, subiculum, CA1 subfield, and CA2/3 subfields. Of note, the dentate gyrus CBV analysis only included slices three–seven because the dentate gyrus did not consistently extend into the first two slices of the anterior region. The anterior–posterior boundary was denoted by the transition between slice four to slice five. The final five hippocampal regions of interest were bilateral hippocampal formation, subiculum, CA1, CA2/3, and dentate gyrus (see Fig. 1 for segmentation in a representative subject). CBV values were generated for each region and used in the statistical analyses.

2.3.3. Statistical analyses

Prior to statistical analyses, data were inspected to detect multivariate outliers; one subject in each group was identified as an outlier and removed from the analytic dataset. The remaining 14 healthy controls and 14 patients were group-matched on age, gender, race, subject education, and parental education (see Table 1). The Positive And Negative Symptom Scale (PANSS) was used to assess patient symptom severity across positive, negative, and general psychopathology (Kay, Fiszbein, and Opler, 1987) and is reported in Table 1. 12 patients were taking a variety of atypical (i.e., aripiprazole, olanzapine, quetiapine, asenapine) and typical (i.e., haloperidol, risperidone, thiothixene) antipsychotic medications at the time of the study. Chlorpromazine equivalent doses were calculated from an international consensus study by Gardner (2010). The chlorpromazine equivalent dose could not be calculated for one subject treated with asenapine, and two subjects were not taking any antipsychotic medications at the time of the study.

To determine whether hemisphere should be included in the model, we performed a preliminary repeated-measures ANOVA to test for hemisphere main effects or interactions. None of the hemisphere tests were significant (all $p > 0.10$); therefore all subsequent analyses were performed on average (left/right) CBV values.

To test the primary hypothesis of diagnosis differences in anterior subfield CBV activity, we performed a repeated-measures ANOVA. Diagnosis was the between-subject factor and subfield (CA1 or CA2/3) was the within-subject factor. Age and gender were matched between groups and were not included as covariates in the ANOVA. We calculated effect sizes (Cohen's d (Cohen, 1988)) and followed up with post-hoc comparisons to aid in interpretation of findings. Post-hoc one-tailed t-tests then investigated group differences in the anterior three slices of the two subfields. As an exploratory analysis, we also tested for group differences in the anterior slices of the subiculum and dentate gyrus. The Statistical Package for Social Sciences software (SPSS Version 20.0. Armonk, NY: IBM Corp.) was used for statistical analyses.
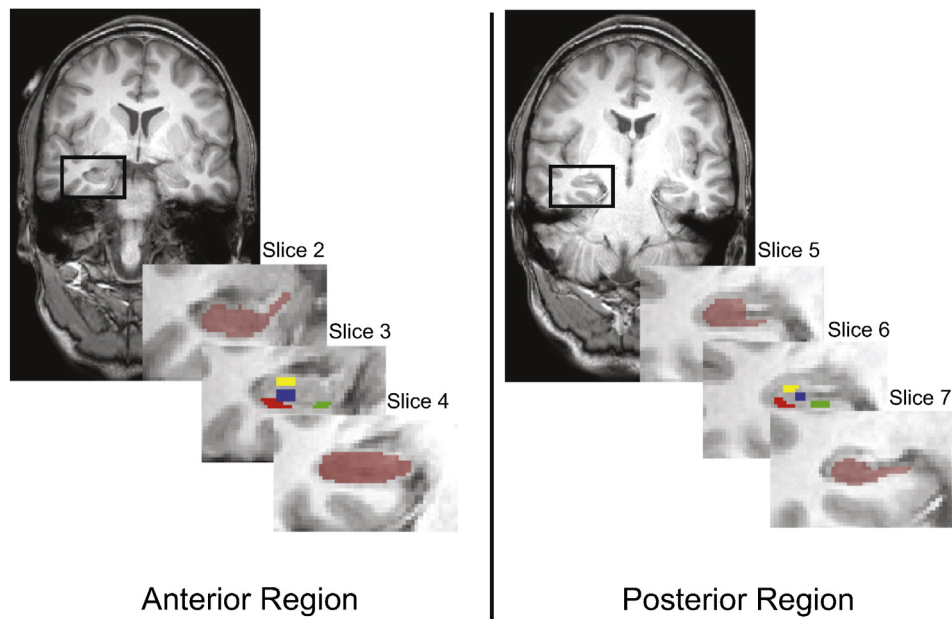
Fig. 1. Manual segmentation of the hippocampal formation and subfields for a representative subject with a structural MRI (radiological orientation). Left: Anterior hippocampal formation (slice 2) outlined in the black box with an inset series of slices through the anterior region. The dark red ROI in slices 2 and 4 illustrates the hippocampal formation ROI while slice 3 denotes the segmented subfields (green = subiculum, red = CA1, yellow = CA2/3, and blue = dentate gyrus). Right: Posterior hippocampal formation (slice 5) outlined in the black box with an inset series of slices through the posterior region. The dark red ROI in slices 5 and 7 illustrates the hippocampal formation ROI while slice 6 denotes the segmented subfields (green = subiculum, red = CA1, yellow = CA2/3, and blue = dentate gyrus).

3. Results

The CBV values ranged from 2.82 to 3.37 (see Table 2) and were similar to values previously reported for the hippocampus (Kuppusamy, 1996).

To test for anterior CA1 versus CA2/3 hyperactivity in schizophrenia, we performed a repeated-measures ANOVA. The resulting analysis showed a diagnosis-by-subfield interaction ($F(1,26) = 5.55$, $p < 0.05$, $d = 0.176$) and no main effect of subfield ($F(1,26) = 2.72$, $p > 0.10$). Healthy controls had significantly lower CBV in CA1 relative to CA2/3 (mean = 2.57 versus mean = 3.07; $F(1,13) = 12.04$, $p < 0.05$). Patients with schizophrenia failed to show this pattern ($p > 0.10$): CBV was similar in CA1 (mean = 2.90) and CA2/3 (mean = 2.81). *Post-hoc* one-tailed *t*-tests within the two subfields revealed a trend for patients with schizophrenia to have increased CBV relative to controls in CA1 ($t(26) = 1.60$, $p = 0.06$, $d = 0.63$; Fig. 2). In contrast, CBV in CA2/3 was slightly decreased in patients with schizophrenia ($p = 0.14$, $d = 0.43$).

To determine whether the subfield-by-diagnosis difference was consistent across the anterior hippocampal formation, or localized within a specific slice, we performed two-sample, one-tailed *t*-tests within each of the three anterior slices. For the CA1 subfield, patients with schizophrenia had increased CBV relative to controls in two of the three slices (see Fig. 3A): slice 2 (trend, $t(25) = 1.591$, $p = 0.06$) and slice 4 ($t(26) = 1.904$, $p < 0.05$). For the CA2/3 subfield, healthy controls had increased CBV relative to patients with schizophrenia in slice 4 (trend, $t(26) = 1.553$, $p = 0.07$, Fig. 3B).

We then performed an exploratory investigation to test for group differences in the anterior subiculum and dentate gyrus. For the subiculum, healthy controls had an average CBV of 4.08, 3.63 and 2.85 for slices 2–4, while patients with schizophrenia had a mean CBV of 4.34, 3.78, and 3.21. *Post-hoc* two-tailed *t*-tests demonstrated no significant group differences (all $p > 0.10$; see Fig. 3C). For the dentate gyrus, healthy controls had an average CBV of 3.44 and 3.03 for slices 2 and 3, while patients had a mean CBV of 3.45 and 3.17. There were no group differences in the dentate gyrus (all $p > 0.10$; see Fig. 3D).

Finally, we tested whether the anterior CA1 CBV correlated with positive, negative, or general psychopathology, or the dose of antipsychotic medication. In the 14 patients, the anterior CA1 CBV did not correlate with positive ($r = 0.18$, $p = 0.53$), negative ($r = -0.12$, $p = 0.69$), or general ($r = -0.03$, $p = 0.91$) psychopathology as assessed by the PANSS. Three of the fourteen patients were not on antipsychotics or the chlorpromazine equivalent dose could not be calculated. Of the remaining 11 patients, there was no significant correlation between dose of antipsychotic medication and anterior CA1 ($r = 0.46$, $p = 0.16$).

4. Discussion

We used high resolution, steady state, contrast-enhanced T1-weighted imaging to test for anterior CA1 versus CA2/3 hippocampal subfield hyperactivity in schizophrenia. Here we report a significant

Table 1

Subject Demographics Fourteen controls and patients with schizophrenia were group-matched on age, gender, race, subject education, and parental education. CPZ denotes chlorpromazine; PANSS denotes Positive and Negative Syndrome Scale.

	Controls (n = 14)	Schizophrenia (n = 14)	Statistic	p-value
Age (yrs ± stdev)	34.57 ± 9.32	32.93 ± 10.89	$t(26) = 0.43$	0.67
Males	9	9	$X^2(1) = 0$	0.65
Race (W/B)	10/4	9/5	$X^2(1) = 0.16$	0.50
Subject Edu. (yrs ± stdev)	15.79 ± 2.69	14.07 ± 2.69	$t(26) = 1.69$	0.10
Avg. Parental Edu. (yrs ± stdev)	14.57 ± 1.86	13.69 ± 2.13	$t(26) = 1.18$	0.25
Duration of Illness (yrs ± stdev)	-	8.47 ± 7.92	-	
CPZ equivalent (mg/day)	-	316.36 ± 170.43	-	
PANSS	-	Positive: 15.93 ± 7.13 Negative: 16.00 ± 6.88 General: 29.64 ± 7.35	-	

Table 2
Cerebral blood volume (CBV) values for each of the 5 regions of interest (ROIs). CBV values (mean ± standard deviation; units = ml blood/ml parenchyma) averaged across hemisphere and along the long axis of the hippocampus for each manually segmented ROI. HF denotes hippocampal formation, and DG denotes dentate gyrus.

	HF	Subiculum	CA1	CA2/3	DG
Control	3.37 ± 0.18	3.11 ± 0.60	2.67 ± 0.16	2.98 ± 0.23	3.18 ± 0.16
Schizophrenia	3.40 ± 0.28	3.29 ± 0.66	2.88 ± 0.15	2.82 ± 0.13	3.09 ± 0.24

diagnosis by subfield interaction due to the combined effect of a trend of increased CA1 CBV ($p = .06$) and non-significantly decreased CA2/3 CBV ($p = 0.14$) in patients relative to healthy controls.

The hippocampal formation integrates multimodal information for the encoding of new and the retrieval of old memories. The entorhinal cortex sends glutamatergic fibers directly to the CA1 subfield (direct pathway) or indirectly to the CA1 subfield via the dentate gyrus and CA3 subfields (indirect pathway) (Amaral, and Witter, 1989). Any dysfunction along these two pathways could lead to increased CA1 CBV. Our results support the hypothesis of increased CA1 CBV in schizophrenia (Schobel, 2009; Schobel, et al., 2013; Small, 2011), but do not support the hypothesis of increased CA3 metabolism in the context of dentate gyrus pathology in schizophrenia (Tamminga, 2012).

Schobel reported increased CBV in the CA1 subfield, which was correlated with positive and negative symptoms of schizophrenia (Schobel, 2009). In a follow-up study, they showed that increased CBV was limited to a single slice in the left anterior CA1 in high-risk patients which spread to the subiculum after psychosis onset (Schobel, et al., 2013). We replicate the CBV increase in schizophrenia selectively in CA1, but do not find it to be limited to the left hemisphere and do not find it to be correlated to positive or negative symptoms.

Shape-based analyses also have reported structural findings in the CA1 subfield. One study in first-episode schizophrenia patients demonstrated regional volume reductions in the left anterior and midbody CA1 (Narr, 2004). Another imaging study has linked left anterior CA1 deformity to antipsychotic dosage and symptom severity in a schizophrenia cohort (Zierhut, 2013). Together, these studies suggest structural and functional alterations in the anterior CA1 in schizophrenia. The CA1 subfield supports novelty detection by comparing information from the indirect pathway (i.e., entorhinal cortex to dentate gyrus to CA3 to CA1) to information received by the direct pathway (i.e., entorhinal cortex to CA1) (Vinogradova, 2001; Knight, 1996; Li, 2003; Lisman, and Otmakhova, 2001). Hippocampal hyperactivity can lead to the formation of delusions and hallucinations through the incorrect formation

and association of memories retrieved by the hippocampal formation (Lisman, 2010; Ewing, and Winter, 2013).

Several mechanisms of disease may lead to hippocampal hyperactivity in schizophrenia. Postmortem and imaging studies have provided support for N-methyl-D-aspartate receptor (NMDAR) hypofunction (Kristiansen, 2007; Théberge, 2002), dopamine dysregulation (Abi-Dargham, 2004; Laruelle, 1999), and gamma-aminobutyric acid-(GABA-)ergic interneuron loss (Akbarian, and Huang, 2006; Konradi, 2011; Nakazawa, 2012; Zhang, and Reynolds, 2002). These three mechanisms have been integrated into a comprehensive model of hippocampal dysfunction in schizophrenia (Lisman, 2008). Hippocampal interneurons are more sensitive than pyramidal neurons to NMDAR blockade (Lisman, 2008; Grunze, 1996; Jones, and Bühl, 1993; Bolton, 2012). In addition, the number of fast-spiking parvalbumin-positive interneurons in CA1 is decreased in schizophrenia (Konradi, 2011). Since hippocampal pyramidal neurons are under tonic inhibition by this interneuron subtype, decreased interneuron function (either through cell loss or pyramidal cell-sensing activity via NMDAR hypofunction) results in the disinhibition of pyramidal neurons in CA1 (which can be registered as increased CBV). In animal models, hyperactivity of CA1 pyramidal neurons results in decreased inhibition of ventral tegmental area (VTA) neurons (Blaha, 1997; Legault, and Wise, 1999; Lodge, 2011), which results in dopaminergic dysfunction and may lead to the positive and negative symptoms of schizophrenia. This prediction is consistent with the finding of CA1 CBV to be correlated positively with delusions and negatively to social dysfunction and avolition in a prodromal cohort (Schobel, 2009). In addition, there is direct evidence that the experience of auditory hallucinations is linked to increased hippocampal activity (using BOLD fMRI (Dierks, 1999) and SPECT with a 99m-Technetium exametazine radiotracer (Musalek, 1989), for review, see (Weiss, and Heckers, 1999)).

We also studied CBV in the subiculum and the dentate gyrus. Since the subiculum serves as the main outflow of the hippocampus, an increase of CBV in CA1 could result in an increase of CBV in the subiculum. Schobel et al. reported increased subiculum CBV at psychosis onset (Schobel, et al., 2013) but, similar to our findings, did not report increased subiculum CBV in chronic schizophrenia patients (Schobel, 2009). This set of results could be due to structural changes in the subiculum after psychosis onset (Rosoklija, 2000). We have recently demonstrated a significant anterior–posterior CBV gradient in the subiculum (Talati, 2014) and further studies are needed to elucidate the role of the subiculum in first-episode psychosis and chronic schizophrenia.

Small sample size is the main limitation of our study and the results should be considered preliminary. But the sample size is comparable to the original study of hippocampal CBV in schizophrenia (18 schizophrenia patients and 18 healthy controls), and we confirm the original finding of increased CA1 CBV (Schobel, 2009) in schizophrenia. We were able to match the control group to the patient group on several parameters, including age, race, and parental education. Most of our patients were treated with antipsychotic medication at the time of the study. However, our studies are consistent with those by Schobel et al. and indicate that antipsychotic medications are not likely to affect resting-state CBV (Schobel, 2009; Schobel, et al., 2013).

In conclusion, we report a subfield by diagnosis interaction due to the combined effect of a trend of increased CA1 CBV ($p = .06$) and non-significantly decreased CA2/3 CBV ($p = 0.14$) in patients relative to healthy controls. Future studies should investigate the evolution of hyperactivity in hippocampal subfields in the early stages of psychosis and their contribution to the generation of the signs and symptoms of psychosis.
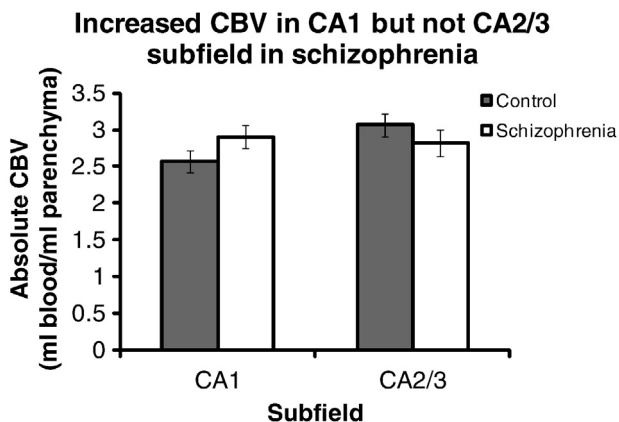

Fig. 2. Increased CBV in the CA1 but not CA2/3 subfield in schizophrenia. For each subject, CA1 or CA2/3 CBV values were collapsed across hemisphere and anterior slices. A repeated-measures ANOVA illustrated a significant diagnosis by slice interaction ($p < 0.05$). A post-hoc one-tailed t-test shows a trend towards increased CBV in the CA1 subfield ($p = 0.06$) but not CA2/3 subfield (p = 0.14). Error bars denote standard error of the mean.
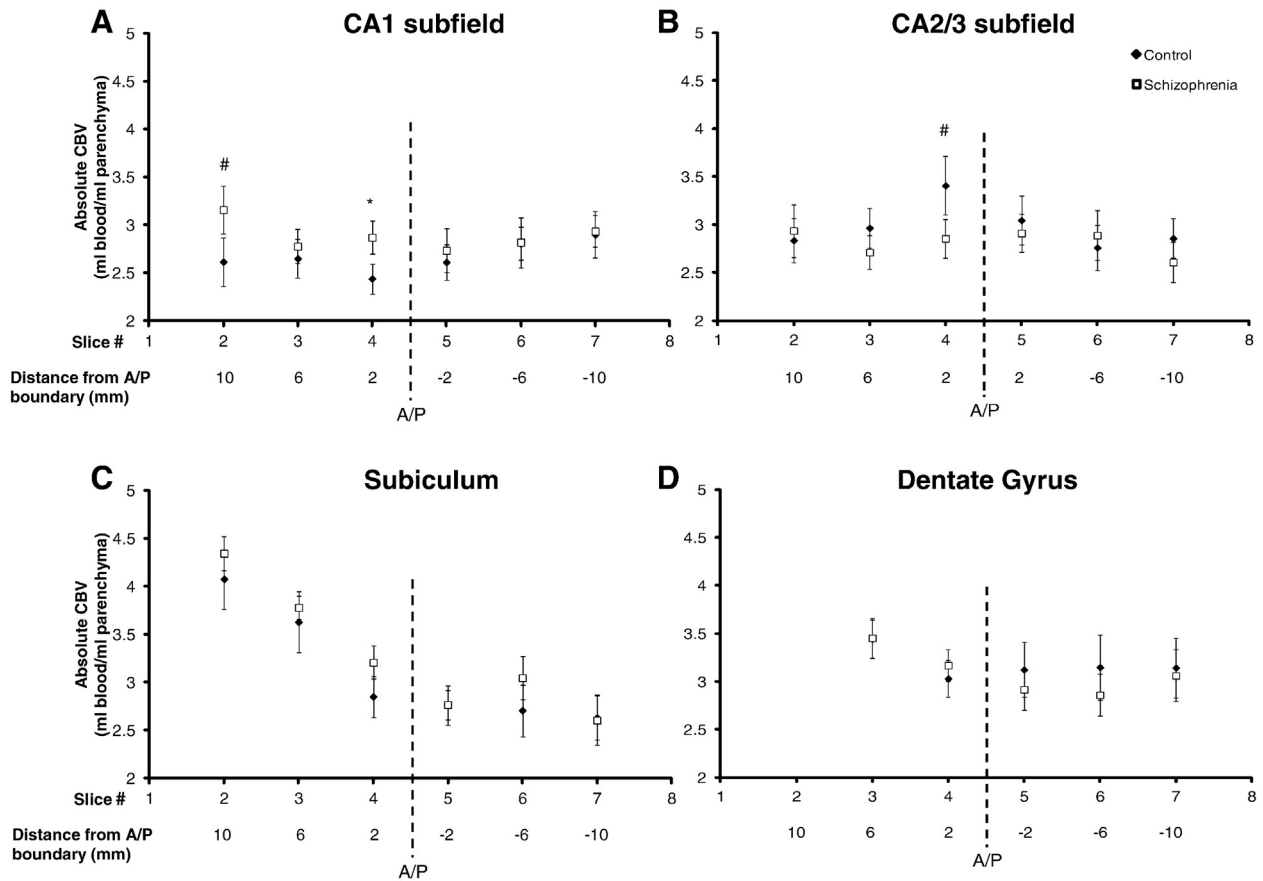
Fig. 3. Increased CBV in the anterior CA1 in schizophrenia. For each subject, subfield CBV values were collapsed across hemisphere for each slice along the long axis of each subfield. *Post-hoc* one-tailed *t*-tests illustrate increased CA1 CBV in slices two ($^{\#} p = 0.06$) and four ($^{*} p < 0.05$) (panel A) and decreased CA2/3 CBV in slice 4 ($^{\#} p = 0.07$) (panel B) in schizophrenia. There were no significant group CBV differences in the subiculum (panel C) and dentate gyrus (panel D). Error bars denote standard error of the mean. A/P refers to anterior/posterior boundary.

the responsibility of the authors and does not necessarily represent the official views of the National Institutes of Health.

References

Abi-Dargham, A., 2004. Do we still believe in the dopamine hypothesis? New data bring new evidence. International Journal of Neuropsychopharmacology 7 (Suppl. 1), S1–S5.

Akbarian, S., Huang, H.S., 2006. Molecular and cellular mechanisms of altered GAD1/GAD67 expression in schizophrenia and related disorders. Brain Research Reviews 52 (2), 293–304. http://dx.doi.org/10.1016/j.brainresrev.2006.04.00116759710.

Aleman, A., et al., 1999. Memory impairment in schizophrenia: a meta-analysis. American Journal of Psychiatry 156 (9), 1358–136610484945.

Amaral, D.G., Witter, M.P., 1989. The three-dimensional organization of the hippocampal formation: a review of anatomical data. Neuroscience 31 (3), 571–5912687721.

Arthurs, O.J., Boniface, S., 2002. How well do we understand the neural origins of the fMRI BOLD signal? Trends in Neurosciences 25 (1), 27–3111801335.

Blaha, C.D., et al., 1997. Stimulation of the ventral subiculum of the hippocampus evokes glutamate receptor-mediated changes in dopamine efflux in the rat nucleus accumbens. European Journal of Neuroscience 9 (5), 902–9119182943.

Bolton, M.M., et al., 2012. Deficits in emotional learning and memory in an animal model of schizophrenia. Behavioural Brain Research 233 (1), 35–44. http://dx.doi.org/10.1016/j.bbr.2012.04.04922569573.

Cohen, J., 1988. Statistical Power Analysis for the Behavioral Sciencessecond edition. L. Erlbaum, Hillsdale, NJ.

Cox, R.W., 1996. AFNI: software for analysis and visualization of functional magnetic resonance neuroimages. Computers and Biomedical Research, an International Journal 29 (3), 162–1738812068.

DeLisi, L.E., et al., 1989. Increased temporal lobe glucose use in chronic schizophrenic patients. Biological Psychiatry 25 (7), 835–8512785820.

Dierks, T., et al., 1999. Activation of Heschl's gyrus during auditory hallucinations. Neuron 22 (3), 615–62110197540.

Duvernoy, H.M., Bourgouin, P., 1998. The Human Hippocampus: Functional Anatomy, Vascularization and Serial Sections with MRI2nd completely rev. and expanded edition. Springer, Berlin, New York.

Ewing, S.G., Winter, C., 2013. The ventral portion of the CA1 region of the hippocampus and the prefrontal cortex as candidate regions for neuromodulation in schizophrenia. Medical Hypotheses 80 (6), 827–832. http://dx.doi.org/10.1016/j.mehy.2013.03.02623583328.

First, M.B., Spitzer, R.L., Miriam, G., Williams, J.B.W., 2002. Structured Clinical Interview for DSM-IV-TR Axis I Disorders, Research VersionResearch Version, Patient Edition With Psychotic Screen (SCID-I/P W/ PSY SCREEN). Biometrics Research, New York State Psychiatric Institute, New York.

Friston, K.J., et al., 1992. The left medial temporal region and schizophrenia. A PET study. Brain: A Journal of Neurology 115, 367–3821606474.

Gardner, D.M., et al., 2010. International consensus study of antipsychotic dosing. American Journal of Psychiatry 167 (6), 686–693. http://dx.doi.org/10.1176/appi.ajp.2009.0906080220360319.

Gloor, P., 1997. The Temporal Lobe and Limbic SystemOxford University Press, New York.

Grunze, H.C., et al., 1996. NMDA-dependent modulation of CA1 local circuit inhibition. Journal of Neuroscience: the Official Journal of the Society for Neuroscience 16 (6), 2034–20438604048.

Gur, R.E., et al., 1995. Resting cerebral glucose metabolism in first-episode and previously treated patients with schizophrenia relates to clinical features. Archives of General Psychiatry 52 (8), 657–6677632119.

Heckers, S., et al., 1998. Impaired recruitment of the hippocampus during conscious recollection in schizophrenia. Nature Neuroscience 1 (4), 318–323. http://dx.doi.org/10.1038/113710195166.

Heckers, S., Konradi, C., 2010. Hippocampal pathology in schizophrenia. Current Topics in Behavioral Neurosciences 4, 529–553.

Heinrichs, R.W., Zakzanis, K.K., 1998. Neurocognitive deficit in schizophrenia: a quantitative review of the evidence. Neuropsychology 12 (3), 426–445. http://dx.doi.org/10.1037/0894-4105.12.3.4269673998.

Jones, R.S., Bühl, E.H., 1993. Basket-like interneurones in layer II of the entorhinal cortex exhibit a powerful NMDA-mediated synaptic excitation. Neuroscience Letters 149 (1), 35–398469376.

Kay, S.R., Fiszbein, A., Opler, L.A., 1987. The positive and negative syndrome scale (PANSS) for schizophrenia. Schizophrenia Bulletin 13 (2), 261–2763616518.

Knight, R., 1996. Contribution of human hippocampal region to novelty detection. Nature 383 (6597), 256–259. http://dx.doi.org/10.1038/383256a08805701.

Konradi, C., et al., 2011. Hippocampal interneurons are abnormal in schizophrenia. Schizophrenia Research 131 (1–3), 165–173. http://dx.doi.org/10.1016/j.schres.2011.06.00721745723.

Kristiansen, L.V., et al., 2007. NMDA receptors and schizophrenia. Current Opinion in Pharmacology 7 (1), 48–55. http://dx.doi.org/10.1016/j.coph.2006.08.01317097347.

Kuppusamy, K., et al., 1996. In vivo regional cerebral blood volume: quantitative assessment with 3D T1-weighted pre- and postcontrast MR imaging. Radiology 201 (1), 106–112. http://dx.doi.org/10.1148/radiology.201.1.88165298816529.

Lahti, A.C., et al., 2003. Functional effects of antipsychotic drugs: comparing clozapine with haloperidol. Biological Psychiatry 53 (7), 601–608 12679238.

Lahti, A.C., et al., 2009. Modulation of limbic circuitry predicts treatment response to antipsychotic medication: a functional imaging study in schizophrenia. Neuropsychopharmacology: Official Publication of the American College of Neuropsychopharmacology 34 (13), 2675–2690. http://dx.doi.org/10.1038/npp.2009.9419675535.

Laruelle, M., et al., 1999. Increased dopamine transmission in schizophrenia: relationship to illness phases. Biological Psychiatry 46 (1), 56–72 10394474.

Ledoux, A.A., et al., 2013. Decreased fMRI activity in the hippocampus of patients with schizophrenia compared to healthy control participants, tested on a wayfinding task in a virtual town. Psychiatry Research 211 (1), 47–56. http://dx.doi.org/10.1016/j.pscychresns.2012.10.00523352276.

Legault, M., Wise, R.A., 1999. Injections of N-methyl-D-aspartate into the ventral hippocampus increase extracellular dopamine in the ventral tegmental area and nucleus accumbens. Synapse (New York, N.Y.) 31 (4), 241–249. http://dx.doi.org/10.1002/(SICI)1098-2396(19990315)31:4<241::AID-SYN1>3.0.CO;2 -#] [Pubmed: 10051104].

Li, S., et al., 2003. Dopamine-dependent facilitation of LTP induction in hippocampal CA1 by exposure to spatial novelty. Nature Neuroscience 6 (5), 526–531. http://dx.doi.org/10.1038/nn104912704392.

Lin, W., Celik, A., Paczynski, R.P., 1999. Regional cerebral blood volume: a comparison of the dynamic imaging and the steady state methods. Journal of Magnetic Resonance Imaging: JMRI 9 (1), 44–52 10030649.

Lisman, J.E., et al., 2010. A thalamo-hippocampal–ventral tegmental area loop may produce the positive feedback that underlies the psychotic break in schizophrenia. Biological Psychiatry 68 (1), 17–24. http://dx.doi.org/10.1016/j.biopsych.2010.04.00720553749.

Lisman, J.E., et al., 2008. Circuit-based framework for understanding neurotransmitter and risk gene interactions in schizophrenia. Trends in Neurosciences 31 (5), 234–242. http://dx.doi.org/10.1016/j.tins.2008.02.00518395805.

Lisman, J.E., Otmakhova, N.A., 2001. Storage, recall, and novelty detection of sequences by the hippocampus: elaborating on the SOCRATIC model to account for normal and aberrant effects of dopamine. Hippocampus 11 (5), 551–568. http://dx.doi.org/10.1002/hipo.107111732708.

Lodge, D.J., Grace, A.A., 2011. Hippocampal dysregulation of dopamine system function and the pathophysiology of schizophrenia. Trends in Pharmacological Sciences 32 (9), 507–513. http://dx.doi.org/10.1016/j.tips.2011.05.00121700346.

Malaspina, D., et al., 2004. Resting neural activity distinguishes subgroups of schizophrenia patients. Biological Psychiatry 56 (12), 931–937. http://dx.doi.org/10.1016/j.biopsych.2004.09.01315601602.

Moreno, H., et al., 2007. Imaging the Abeta-related neurotoxicity of Alzheimer disease. Archives of Neurology 64 (10), 1467–1477. http://dx.doi.org/10.1001/archneur.64.10.146717923630.

Musalek, M., et al., 1989. Regional brain function in hallucinations: a study of regional cerebral blood flow with 99m-Tc-HMPAO-SPECT in patients with auditory hallucinations, tactile hallucinations, and normal controls. Comprehensive Psychiatry 30 (1), 99108 2784369].

Nakazawa, K., et al., 2012. GABAergic interneuron origin of schizophrenia pathophysiology. Neuropharmacology 62 (3), 1574–1583. http://dx.doi.org/10.1016/j.neuropharm.2011.01.02221277876.

Narr, K.L., et al., 2004. Regional specificity of hippocampal volume reductions in first-episode schizophrenia. NeuroImage 21 (4), 1563–1575. http://dx.doi.org/10.1016/j.neuroimage.2003.11.01115050580.

Nordahl, T.E., et al., 1996. Temporal lobe metabolic differences in medication-free outpatients with schizophrenia via the PET-600. Neuropsychopharmacology: Official

Publication of the American College of Neuropsychopharmacology 15 (6), 541–554. http://dx.doi.org/10.1016/S0893-133X(96)00098-X8946428.

Ongür, D., et al., 2006. The neural basis of relational memory deficits in schizophrenia. Archives of General Psychiatry 63 (4), 356–365. http://dx.doi.org/10.1001/archpsyc.63.4.35616585464.

Ragland, J.D., et al., 2001. Effect of schizophrenia on frontotemporal activity during word encoding and recognition: a PET cerebral blood flow study. American Journal of Psychiatry 158 (7), 1114–1125 11431234.

Rosoklija, G., et al., 2000. Structural abnormalities of subicular dendrites in subjects with schizophrenia and mood disorders: Preliminary findings. Archives of General Psychiatry 57 (4), 349–356 10768696.

Schobel, S.A., et al., 2009. Differential targeting of the CA1 subfield of the hippocampal formation by schizophrenia and related psychotic disorders. Archives of General Psychiatry 66 (9), 938–946. http://dx.doi.org/10.1001/archgenpsychiatry.2009.11519736350.

Schobel, S.A., et al., 2013. Imaging patients with psychosis and a mouse model establishes a spreading pattern of hippocampal dysfunction and implicates glutamate as a driver. Neuron 78 (1), 81–93 23583108.

Small, S.A., et al., 2011. A pathophysiological framework of hippocampal dysfunction in ageing and disease. Nature Reviews. Neuroscience 12 (10), 585–601. http://dx.doi.org/10.1038/nrn308521897434.

Talati, P., et al., 2014. Anterior–posterior cerebral blood volume gradient in human subiculum. Hippocampus 24 (5), 503–509. http://dx.doi.org/10.1002/hipo.2225724677295.

Tamminga, C.A., et al., 2012. Glutamate dysfunction in hippocampus: relevance of dentate gyrus and CA3 signaling. Schizophrenia Bulletin 38 (5), 927–935. http://dx.doi.org/10.1093/schbul/sbs06222532703.

Tamminga, C.A., et al., 1992. Limbic system abnormalities identified in schizophrenia using positron emission tomography with fluorodeoxyglucose and neocortical alterations with deficit syndrome. Archives of General Psychiatry 49 (7), 522–530 1627043.

Tamminga, C.A., Stan, A.D., Wagner, A.D., 2010. The hippocampal formation in schizophrenia. American Journal of Psychiatry 167 (10), 1178–1193. http://dx.doi.org/10.1176/appi.ajp.2010.0908118720810471.

Théberge, J., et al., 2002. Glutamate and glutamine measured with 4.0 T proton MRS in never-treated patients with schizophrenia and healthy volunteers. American Journal of Psychiatry 159 (11), 1944–1946 12411236.

Tregellas, J.R., et al., 2014. Intrinsic hippocampal activity as a biomarker for cognition and symptoms in schizophrenia. American Journal of Psychiatry 171 (5), 549–556. http://dx.doi.org/10.1176/appi.ajp.2013.1307098124435071.

Tregellas, J.R., 2014. Neuroimaging biomarkers for early drug development in schizophrenia. Biological Psychiatry 76, 111–119. http://dx.doi.org/10.1016/j.biopsych.2013.08.02524094513.

Vinogradova, O.S., 2001. Hippocampus as comparator: role of the two input and two output systems of the hippocampus in selection and registration of information. Hippocampus 11 (5), 578–598. http://dx.doi.org/10.1002/hipo.107311732710.

Weiss, A.P., et al., 2003. Impaired hippocampal recruitment during normal modulation of memory performance in schizophrenia. Biological Psychiatry 53 (1), 48–55 12513944.

Weiss, A.P., Heckers, S., 1999. Neuroimaging of hallucinations: a review of the literature. Psychiatry Research 92 (2–3), 61–74 10674360.

Woolard, A.A., Heckers, S., 2012. Anatomical and functional correlates of human hippocampal volume asymmetry. Psychiatry Research 201 (1), 48–53. http://dx.doi.org/10.1016/j.pscychresns.2011.07.01622025719.

Zhang, Z.J., Reynolds, G.P., 2002. A selective decrease in the relative density of parvalbumin-immunoreactive neurons in the hippocampus in schizophrenia. Schizophrenia Research 55 (1–2), 1–10 11955958.

Zierhut, K.C., et al., 2013. Hippocampal CA1 deformity is related to symptom severity and antipsychotic dosage in schizophrenia. Brain: A Journal of Neurology 136 (3), 804–814. http://dx.doi.org/10.1093/brain/aws33523388407.